Registration No: 170170725

The University of Sheffield
Electrical and Electronic Engineering

Bipolar Junction Transistor – Lab Report

Professor Geraint Jewell

21/02/2018

1 Contents

2 Introduction

The Bipolar Junction Transistor (BJT) Laboratory aims to give students the opportunity the practically investigate and understand the operation of BJTs. The electrical characteristics of the BC549B BJT [1] will be measured and plotted; they can then be used to generate a small signal model. Once a small signal model of the BJT has been generated it can be used to calculate component values that will set up the ideal biasing conditions for a single stage audio amplifier.

The ideal single stage amplifier will be constructed using the component values calculated from the small signal model. The amplifier performance will then be tested so that its real-world characteristics can be compared to those produced by the small signal model. Ultimately this should give students insight into the practical limitations of BJT devices and their use in amplification circuits.

3 Background, Theory and Method

These sections are not required for this report, further information can be found in the EEE118 module lecture notes found on the MOLE webpage or the Bipolar Junction Transistor Laboratory Script [2].

4 Results

This section covers the results from the testing of the BJT electrical characteristics and the performance of the single stage amplifier constructed using values generated by the small signal model. The physical characteristics of the transistor will also be briefly discussed.

4.1 BC549B BJT Physical Characteristics

The datasheet was used to identify that the BC549B BJT is an NPN transistor as well as to find the pin configuration of the device. The diode test function on the Digital Multimeter (DMM) was then used to confirm this. Results from this experiment are shown in **Figure 4.1**.

Pin 1	Pin 2	Prediction	Result
Base	Collector	Forward Biased	Forward Biased
Base	Emitter	Forward Biased	Forward Biased
Collector	Base	Reverse Biased	Reverse Biased
Collector	Emitter	Reverse Biased	Reverse Biased
Emitter	Base	Reverse Biased	Reverse Biased
Emitter	Collector	Reverse Biased	Reverse Biased

Figure 4.1: Electrode Identification Test Chart

4.2 BC549B BJT Electrical Characteristics

A DC Power Supply was used in conjunction with the University of Sheffield's custom BJT Lab circuit board to characterise the input, output and transfer electrical characteristics of the BC549B BJT. The output characteristic graph is shown in **Figure 4.2**. The Collector Emitter Voltage vs Collector Current curve is shown for each set Base Current. The Load Line used for the setup of the Small Signal Model is shown as a black line, the known DC and zero Collector Current conditions points used to construct this load line are shown as red dots. Finally, the load line of the system when a set of headphones is connected to the output is shown as a dashed red line.

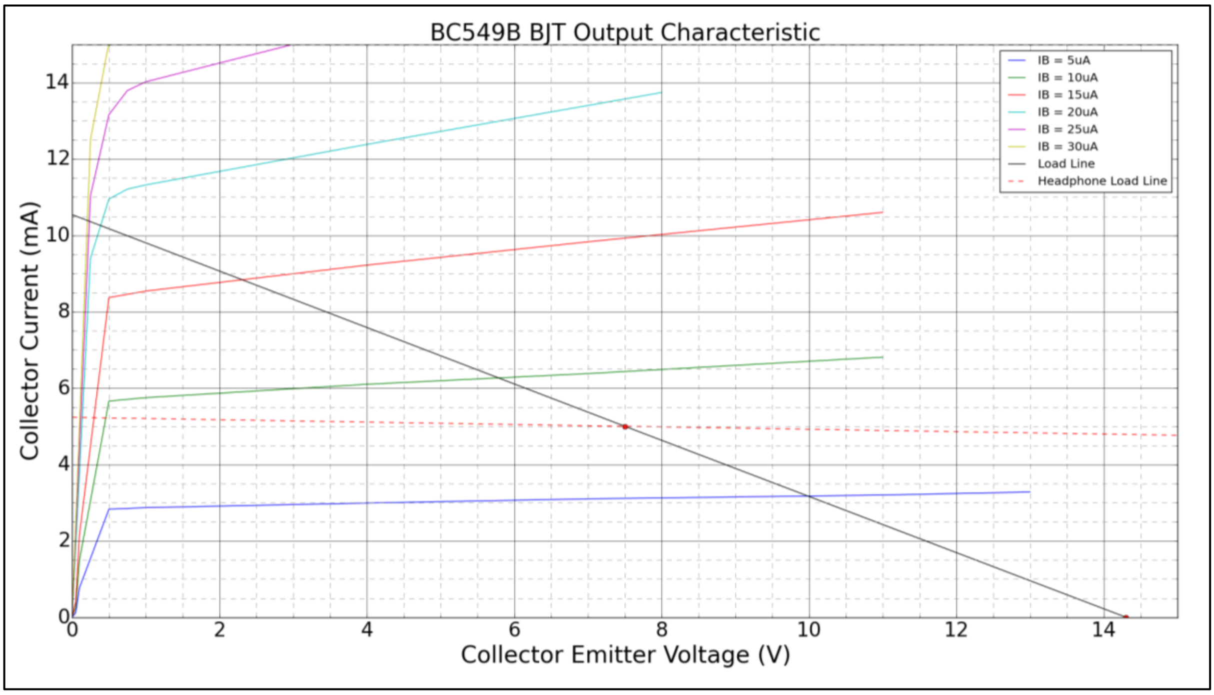

Figure 4.2: BC549B BJT Output Characteristics (generated using Python XY [5])

The transfer characteristic graph is shown in **Figure 4.3**. The experimental transfer characteristic results are shown as red dots with the regression curve as a green line. The tangent line used to calculate the transconductance in the small signal model is shown in blue. Finally, the lines used to calculate the Base Voltage at the stated quiescent Collector Current of 5mA [2] are shown as dashed red lines.

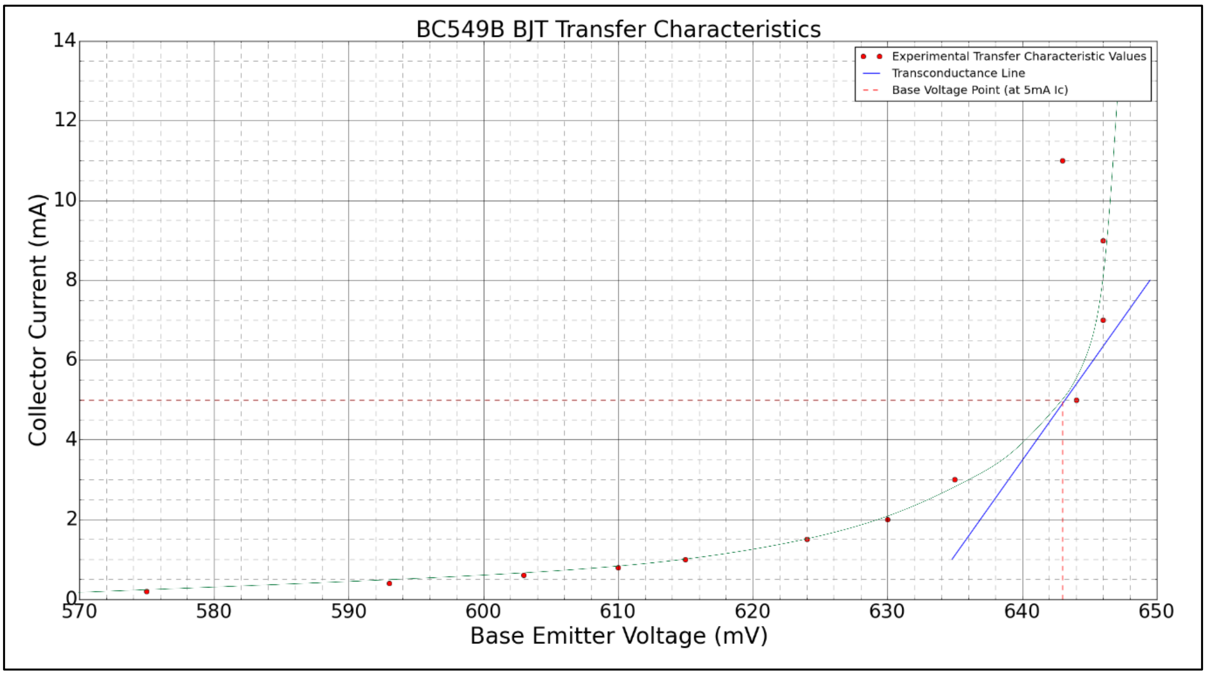

Figure 4.3: BC549B BJT Transfer Characteristics (generated using Python XY [5])

Finally, the input characteristic graph is shown in **Figure 4.4**. The experimental input characteristic results are shown as red dots with the regression curve shown as a green line. The tangent line used to calculate the Base Emitter resistance in the small signal model is shown in blue. Finally, the lines used to calculate the Base Current at the stated quiescent Collector Current of 5mA [2] are shown as dashed red lines.

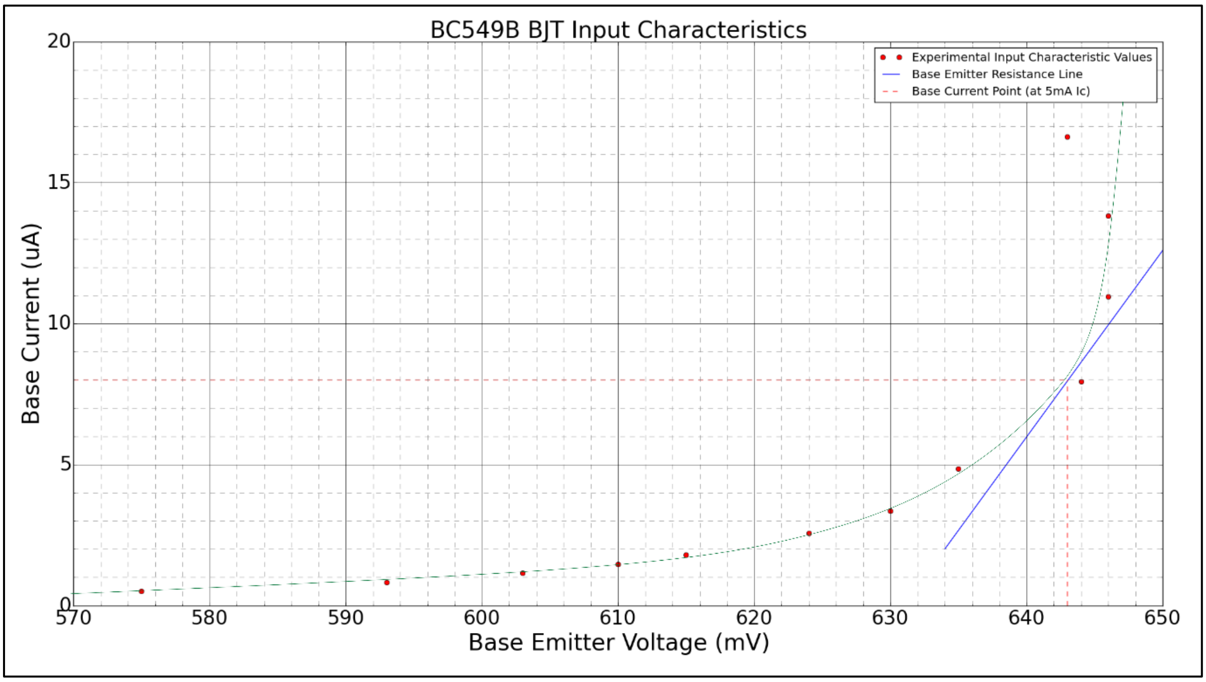

Figure 4.4: BC549B BJT Input Characteristic (generated in Python XY [5])

4.3 Single Stage Amplifier Performance

Using the small signal model constructed from the experimental results from the electrical characteristics testing outlined in section **4.2** a set of bias resistor values was calculated. **Figure 4.5** compares these calculated resistor values to the values provided in the lab.

Resistor Name	R1	R2
Calculated Value (kΩ)	85.7	8.9
Measured Value (kΩ)	68.16	7.33

Figure 4.5: Bias Resistor Values

Using a Bench Power Supply and DMM the DC Conditions of the biased single stage amplifier circuit were measured. These measured DC conditions are compared to the DC conditions calculated using the small signal model in **Figure 4.6**.

Single Stage Amplifier DC Conditions				
	Base Emitter Voltage (mV)	Base Current (μA)	Collector Current (mA)	Collector Emitter Voltage (V)
Calculated	643	8	5	7.5
Measured	638	13.76	9.28	7.5

Figure 4.6: Single Stage Amplifier DC Conditions

Using a Waveform Generator set to output a 2Vpp 10kHz Sine Wave and a DMM the AC output characteristics of the single stage amplifier were measured. These measured values were then used to calculate the actual voltage gain of the circuit, which could then be compared to the theoretical gain value calculated using the small signal model. The calculated and measured values can be seen in **Figure 4.7**. It is also important to note that the Input and Output signals were observed to be 180° out of phase with each other.

Single Stage Amplifier AC Output Characteristics			
	Vin (mV)	Vout (V)	Voltage Gain (Vout/Vin)
Calculated	2.7	2	740.7
Measured	14	1.95	139.3

Figure 4.7: Single Stage Amplifier AC Output Characteristics

Figure 4.8 and **Figure 4.9** show the Collector Emitter Voltage Waveform and Base Current Waveform respectively that was produced when the AC signal was inputted into the single stage amplifier. The DC Conditions for each waveform are shown by a dashed red line. These graphs confirm the observation that the input and output signals are 180° out of phase. In both cases one full cycle of the signal is shown.

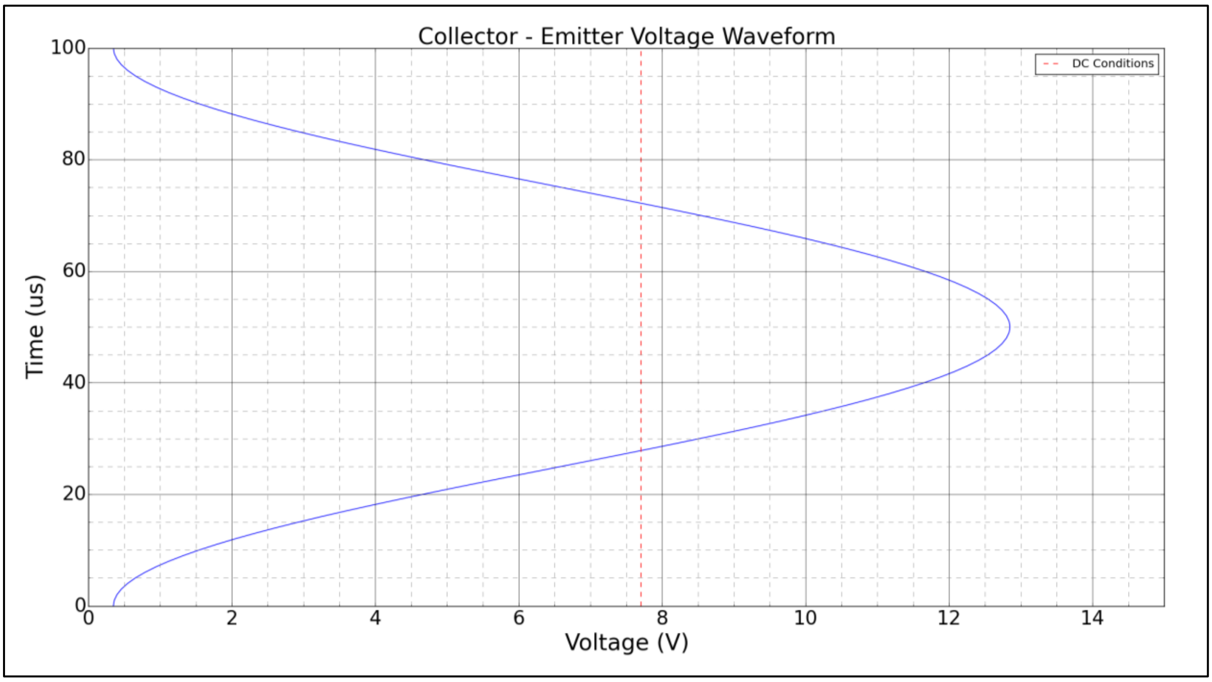

Figure 4.8: Collector Emitter Voltage Waveform from AC Input

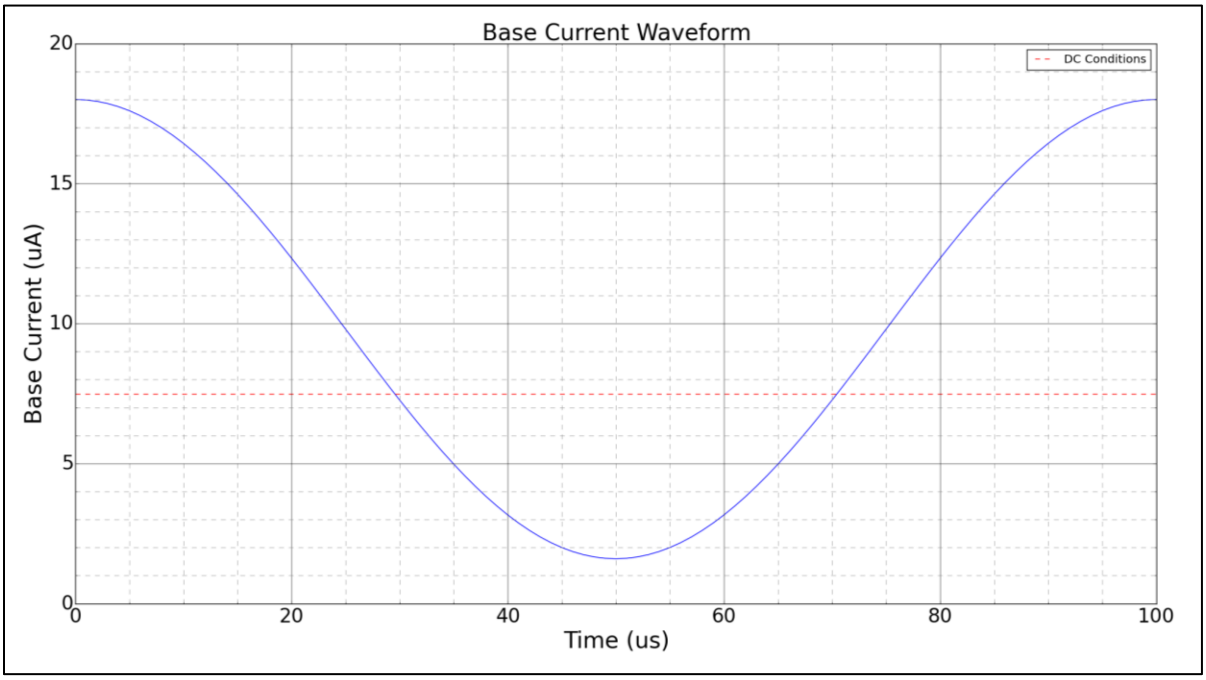

Figure 4.9: Base Current Waveform from AC Input

4.4 AC Effects on the Load Line (Headphones)

A set of 32Ω impedance headphones was connected to the output of the audio amplifier, the input Voltage and Output Voltage of the single stage amplifier were then measured. These voltages were used to calculate the amplifiers gain with a load attached to the output. The results from this experiment are shown in **Figure 4.10**. The change in the load line of the circuit can be observed in **Figure 4.2**.

AC Effects on the Load Line - Gain Calculation with loaded Output		
Vin (mV)	Vout (mV)	Voltage Gain (Vout/Vin)
14	90	6.43

Figure 4.10: Gain Calculation with a loaded amplifier Output

5 Discussion

5.1 BJT Electrical Characteristics

The output characteristic graph generated using the electrical characteristic testing (shown in **Figure 4.2**) allows the calculation of the device DC Gain (h_{fe}) and thus the device Current Gain (β) at low frequencies. A β of 680 was calculated from the output characteristic graph, whilst the manufacturers datasheet gives a range of 200 – 450 for the BC549B BJT [1]. This wide disparity between the calculated Current Gain and the specified Current Gain eludes to two of the key issues of amplifier construction with BJT devices.

Firstly, the manufacturers specification provides a wide range of possible current gain values, making it difficult for an engineer to correctly design a biasing circuit to obtain optimal amplifier performance (low distortion, wide frequency response, high voltage gain). Β is difficult to control during transistor production as it is heavily affected by the doping density and width of the transistor base [2].

Secondly, given that the calculated value of Current Gain from the small signal model is well outside the manufactures specification, the small signal model clearly produces results that cannot be easily and repeatably replicated in the real world. This is largely due to the Current Gain being affected by both transistor temperature and collector current [3, p. 91]. Current Gain is not a constant value and shows a non-linear increase with collector current and temperature.

The output characteristic graph also shows us that, in line with the theory covered in module EEE118, the maximum collector current increases proportionally to the supplied base current (approximately a 5mA increase in maximum collector current with a 10μA increase in base current). This shows that the BJT can be treated as a current amplification device.

The transfer characteristic graph (shown in **Figure 4.3**) shows that, at a constant collector emitter voltage, the collector current increases exponentially with base emitter voltage. Thus, in line with the theory covered in module EEE118, the collector current increases proportionally with the base emitter voltage.

Figure 4.3 also shows the tangent line used to calculate the BJT transconductance as given by the experimental data. This tangent line gives a transconductance value of 0.483, whereas theoretical calculations [3, p. 92 Eq 2.13] give a transconductance value of 0.192. This backs up the earlier conclusion as to the inaccuracy of the small signal model due to the non-linear nature of the BJT transconductance.

The input characteristic graph (shown in **Figure 4.4**) shows that, at a constant collector emitter voltage, the base current of the BJT increases exponentially with the base emitter voltage. This confirms that the base emitter path has a finite resistance, as per the theory from module EEE118. However, it also shows that this finite resistance is not ohmic in behaviour. This correlates with theoretical predictions that state the base emitter resistance is proportional to the collector current and temperature [3, p. 92 Eq 2.12].

Finally, **Figure 4.4** shows the tangent line used to calculate the measured base emitter resistance. This tangent line gives a base emitter resistance of $6.5\times10^{-4}\Omega$; this is in stark contrast to theoretical predictions [2, p. 16 Eq 2] which give a range of 1041 – 2343Ω for the β range of 200 – 450 stated in the device datasheet [1].

5.2 Single Stage Amplifier Performance

Theoretically the calculated values produced by the small signal model using the experimental data discussed in section **4.2** and **5.1** can be used to produce resistance values that will correctly bias the BJT base to produce optimal single stage amplifier performance. This presents the usage case of these graphs; as they are usually provided within the device datasheet they can be used to produce circuit schematics without prior device testing.

In practice, this is not the case for the single stage amplifier design used in this experiment due to the issues discussed in section **5.1**. The wide range of device current gain characteristics and inaccuracy of the small signal model due to the non-linearity of device transconductance and base emitter resistance make it very difficult to design circuits with this structure that will produce repeatable results for gain, frequency response and distortion. As such they are difficult to use in commercialised products.

These conclusions are backed up by the results presented in **Figure 4.6** and **Figure 4.7**. **Figure 4.6** shows a difference in DC Base Current of 5.76μA (8μA Calculated, 13.76μA Measured) and a difference in Collector Current of 4.28mA (5mA Calculated, 9.28mA Measured). These errors are most likely due to the difference in bias resistance values used as presented in **Figure 4.5** and the temperature coefficient of the resistors used inducing changes in the bias voltage at different collector and base currents.

Figure 4.7 shows that the calculated Voltage Gain for the AC Output Characteristics was 5.32 times greater than the measured Voltage Gain from the AC Output Characteristics test. This will be caused by the non-linearity of the BJT current gain and base emitter resistance causing a much higher input voltage to be required for the same change in output voltage.

Figure 4.8 and **Figure 4.9** show the output voltage and input current waveforms respectively. These figures show that the waveforms produced by the amplifier are not centred around the DC operating point. Consequently, the amplifier will amplify a greater amplitude of signal in the negative direction without distortion than in the positive direction. This is particularly important in audio amplifier applications where the audio signal will not distort evenly across the hearable frequency range, for example making the bass of a song very distorted whilst the highs are very clear.

Ultimately, circuit designers must use circuit designs such as matched biasing transistors [3, p. 97] to compensate for these variations in transistor characteristics. Simple single stage amplifier designs such as the one used in this experiment are simply not suitable for modern commercial use due to their low reliability and output repeatability across manufactured circuits. This largely explains the common use of Operation Amplifiers in modern analogue circuits due to their low temperature dependence, high input impedance and extremely high gain, not to mention their comparatively low part cost considering their functionality.

5.3 AC Effects on Load Line (Headphone Load)

Finally, **Figure 4.10** shows the effect of loading the amplifier output, in this case with a pair of 32Ω headphones. In this case the Voltage Gain is significantly decreased from 139.3 to 6.43. This shows that the amplification of the circuit is directly affected by the output load; the higher the load, the lower the circuit amplification.

This is unacceptable for most applications where the aim is to keep the gain constant with load. For example, this would result in a different level of audio volume being available depending on the impedance of the headphones used with the audio amplifier. In this case, a pair of 180Ω headphones would render the audio almost inaudible due to the low levels of amplification achieved by the circuit.

5.4 Measurement Errors

The largest source of error in these experiments (apart from the large range of transistor characteristics discussed previously) is the use of the Tenma Hand Held DMM in the measurement of the Collector Emitter Voltage. These DMM units have an AC RMS Voltage accuracy of ±(1.2% + 1V) when set to the 200V range [4, p. 29]. Despite this large error in AC RMS Voltage reading, it has limited effect on our conclusions as it does not account for the extremely large discrepancies between the calculated and measured transistor characteristic values. This is largely due to it not being used for measurements that required a high level of resolution and accuracy, as per the laboratory method [2].

6 Conclusion

In conclusion, we have successfully investigated the behaviour of BJTs and shown that their behaviour correlates with the theory outlined in module EEE118 through **Figure 4.2, Figure 4.3** and **Figure 4.4**.

The characteristics of the BJT have been measured through a series of tests for output, input and transfer characteristics. These measurements were plotted to produce values of 0.483, $6.5\times10^{-4}\Omega$ and 680 for transconductance, base emitter resistance and current gain respectively. These values were compared to the values given by theoretical transistor models [3] (g_m = 0.192, β = 200 – 450, r_{be} = 1041 – 2343) to show the large error in results produced by the small signal model.

The measured values from the transistor characteristic graphs were used to produce a single stage audio amplifier design with the intended ideal DC conditions. Testing was completed (**Figure 4.6** and **Figure 4.7**) to show the large discrepancy between the predicted voltage gain of 740.7 and the measured voltage gain of 139.3. The difference in predicted and measured DC conditions was also shown to produce an uneven voltage swing between the amplifier supply voltages, increasing signal distortion in the positive direction.

Ultimately this showed that the significant variations in BJT characteristics from device to device and the inaccuracy of predictions from the small signal model due to device current gain, transconductance and base emitter resistance non-linearity makes it extremely difficult to produce an BJT amplifier that has repeatable characteristics. This explains the wide use of operational amplifiers in modern amplification circuits due to their high input impedance, low output impedance, wide frequency response and high gain.

Finally, the effects of loading the single stage amplifier were tested using a pair of 32Ω headphones. It was shown (**Figure 4.10**) that the loading of the amplifier output significantly reduced the system voltage gain from 139.3 to 6.43. Again, this is an undesirable characteristic in audio amplifier applications as this would render some sounds inaudible and reduce the clarity of the audio signal.

7 References

[1] ON Semiconductor, "BC549B Datasheet," 11 2014. [Online]. Available: https://www.mouser.com/ds/2/308/BC549-1118579.pdf. [Accessed 21 02 2018].

[2] The University of Sheffield, "Bipolar Junction Transistor," Sheffield, 2018.

[3] P. Horowitz and W. Hill, The Art of Electronics, 3 ed., New York, NY: Cambridge University Press, 2015.

[4] Tenma, "Tenma 72-7770 Datasheet," [Online]. Available: https://vle.shef.ac.uk/webapps/blackboard/execute/content/file?cmd=view&content_id=_3016876_1&course_id=_68905_1. [Accessed 21 02 2018].

[5] P. Raybaut and G. Davar, "Python XY," [Online]. Available: https://python-xy.github.io/.

8 Appendices

Output Characteristic Data Table											
Base Current											
5uA		10uA		15uA		20uA		25uA		30uA	
Vce (V)	Ic (mA)	Vce (V)	Ic (mA)	Vce (V)	Ic (mA)	Vce (V)	Ic (mA)	Vce (V)	Ic (mA)	Vce (V)	Ic (mA)
0	0	0	0	0	0	0	0	0	0	0	0
0.05	0.12	0.05	0.26	0.05	0.41	0.25	9.4	0.25	11.04	0.25	12.51
0.1	0.77	0.1	1.49	0.1	2.16	0.5	10.95	0.5	13.16	0.5	15.04
0.5	2.83	0.5	5.66	0.5	8.37	0.75	11.21	0.75	13.79	0.75	16.24
1	2.87	1	5.75	1	8.54	1	11.32	1	14.02	1	16.56
4	2.99	4	6.1	4	9.22	4	12.38	4	15.49	4	18.49
7	3.1	7	6.38	7	9.83	8	13.74	7	16.81	6	19.75
11	3.2	11	6.81	11	10.6						
13	3.28										

Figure 8.1: Output Characteristic Data Table

Transfer and Input Characteristic Data Table			
Ic (mA)	Vce (V)	Ib (uA)	Vbe (mV)
0	7.5	0.21	0
0.1	7.5	0.36	560
0.2	7.5	0.52	575
0.4	7.5	0.83	593
0.6	7.5	1.16	603
0.8	7.5	1.47	610
1	7.5	1.79	615
1.5	7.5	2.56	624
2	7.5	3.36	630
3	7.5	4.86	635
5	7.5	7.95	644
7	7.5	10.95	646
9	7.5	13.83	646
11	7.5	16.62	643
13	7.5	19.43	641

Figure 8.2: Transfer and Input Characteristic Data Table